

Seismic Demands of the Case Study Highway Bridge under Near Fault Pulse-Like Ground Motion



A. Dolati, T. Taghikhany & A. Rahai
Amirkabir University of Technology (Polytechnic of Tehran), Iran

SUMMARY

Effect of near fault pulse-like ground motions on seismic demand of Highway Bridges is a complicated process which depends on several parameters such as source-to-site geometry, ground motion amplitude and so on. Herein, an existing regular box girder Highway Bridge in Iran has been considered as a case study. This real model developed to five extra ones for further study and considering irregularity according to the criteria of AASHTO 2007 provision in spans and pier's height ratios (stiffness). Three-dimensional nonlinear model of the bridges have been built through OpenSees software and excited under two sets of near fault and far fault earthquakes. The results indicate that near fault pulse like ground motions have more severe effects on both directions of bridges in compare with far fault ones. Additionally, comparing the responses of different bridges exhibits that the irregular bridges under near fault earthquakes are most affected.

Keywords: Post-tensioned concrete bridges, Near Fault ground motions, Forward directivity.

1. INTRODUCTION

After extensive damages observed in engineering designed structures at vicinity of seismic sources (Bertero et al. 1978, Alavi and Krawinkler 2001), many researches have been conducted towards studying on nature of ground motion in the close distance of causative fault. Their results indicate that because of the way that rupture propagates and energy releases, ground motions close to the ruptured fault can be significantly different than those further away from the seismic source. The most important characteristics which is forward directivity, occurs in fault normal components and causes large amplitude pulse at beginning of the record and contains most of the record's energy (Somerville 2003). The effect of forward directivity is decreased with distance from the fault as seismic waves scatter, such that near-fault pulse-like ground motions are unlikely to be occurred in more than 10 to 15 km away from the rupture (Iervolino and Cornell 2008).

The similar researches have shown the role of pulse-like ground motions on seismic damages of important infrastructures such as highway bridges. Liao et al. (2000) declared higher values of ductility and deformation demands of a five spans bridge under near fault pulse like ground motion. Phan et al. (2007) conducted experimental dynamic test on bridge piers and their outcomes indicate on large residual deformation of piers under near fault ground motions. Their test results demonstrated that the residual deformations of piers under one directional near fault pulses are more than ordinary bi-directional pulses. Also Kalkan et al. (2006) compared the hysteretic energies of structures under near fault in compare with far fault ground motions. Their analysis denoted on high deformation demand with low hysteretic energy of structural elements under near fault ground motion.

Most of researches on seismic performance of highway bridges under near fault strong motions are focused on specific scenario and type of structures. Herein, to have general prospect regarding to seismic performance of highway bridges, a case study framed box girder Highway Bridge is investigated by using a three dimensional precise model. Furthermore, for evaluating the effect of irregularity, five extra bridges have been designed by altering dimensions in case study bridge and drag in irregularity of its spans and pier heights according to AASHTO 2007 provision. Three dimensional models of bridges assist to capture four different scenarios of near fault ground motions in compare to far fault ones in DBE and MCE level. The scenarios have been chosen based on fault rupture direction regarding to bridge position in order to study forward directivity pulses in each direction of piers. The generated 3D nonlinear models in OpenSees were subjected by set of pulse like near fault ground motions. The near fault ground motions are selected to cover wide range of pulse periods recoded on soil type II. The seismic demand parameters like drift ratio, hysteretic energy related to input energy and damage index (DI) of piers in different scenarios were computed in longitudinal and transverse direction.

2. DESCRIPTION OF ANALYTICAL REGULAR AND IRREGULAR BRIDGES

In order to provide a comprehensive study, a case study bridge as a reference model has been selected. This model is a segmental precast post tensioned viaduct which (See Fig. 2.1). Its continuous none prismatic deck has total length of 215 meters with three spans of 60, 95 and 60 meters. The deck is post tensioned with pre-stress force of 157.68 ton.

Two piers of bridge are prismatic and have equal height of 22.7 meters. Their rectangular section's dimension is 1.5x4.5 meters with average axial index (Eqn. 2.1) of 12.0% (See Fig. 2.1). The PMM ratio in critical sections is about 0.80 and transverse bars in piers were chosen how the maximum shear demands of plastic hinges do not control the performance of piers. With the specifications which have been illustrated, the bridge is considered as regular according to AASHTO 2007 provisions.

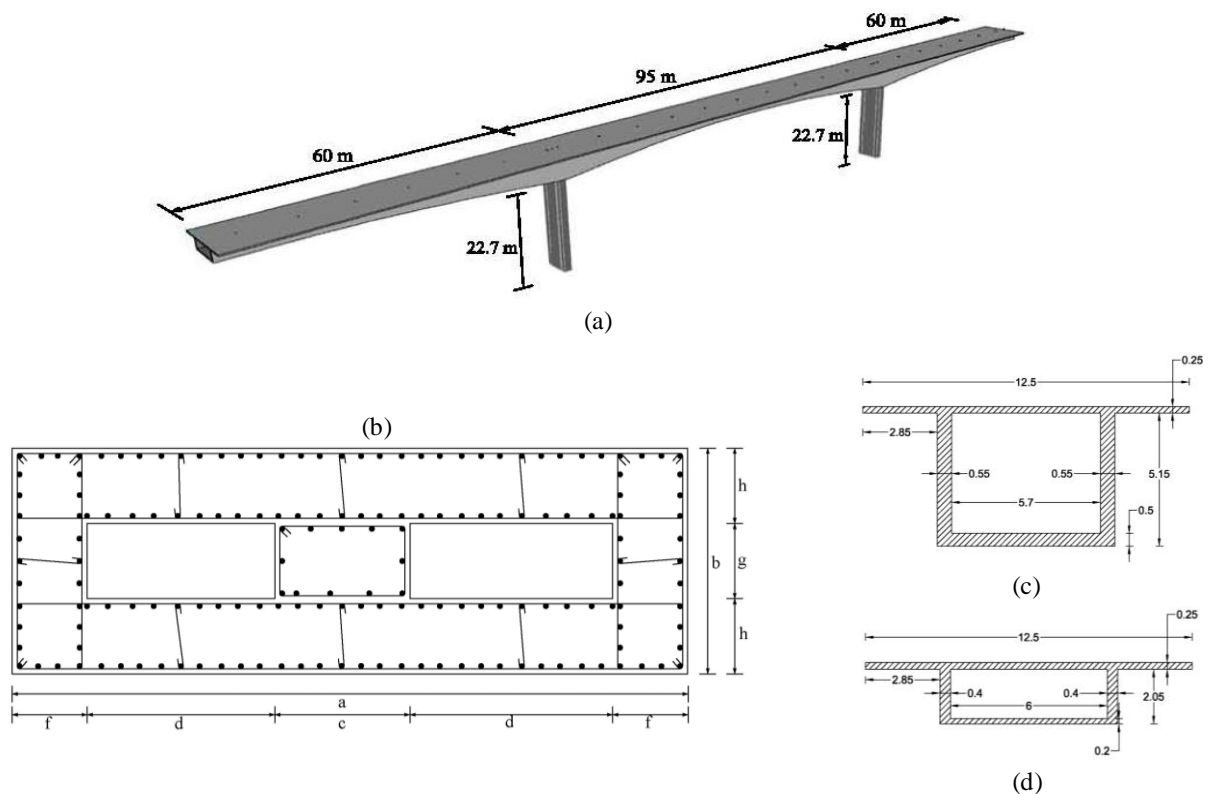


Figure 2.1. Three span case study regular bridge (a) general view, (b) piers cross section, (c) deck sections at top of the piers and (d) deck section at span

Fig. 2.2 shows six different models considered in this study. In order to have unique and comparable results, the pier's dimensions and number of its longitudinal bars have been chosen how the axial index (AI) and DCR ratio would be the same value in all piers. Axial index (AI) is calculated from Eqn. 2.1 (Sadrossadat zadeh and Saiidi 2007). In this equation P is axial load due to dead load plus half of live load, f'_c is compressional strength of the concrete and A_g is gross section of the pier.

$$AI = \frac{P}{f'_c A_g} \quad (2.1)$$

Table 2.1 provides the relative stiffness of piers in generated irregular models. As it is shown, models No. 2 and 5 represents span ratio irregularity and models No. 3 and 6 have irregularity in pier's stiffness (height of piers). In all designed models in order to justifying DCR ratio, the percent of longitudinal ratios were changed, while dimensions of piers were kept the same as the regular bridge. There was an exception in model No 5 (span irregularity), where the left pier's dimension and its stiffness ratio have been changed due to considerable reduction in contributed vertical load.

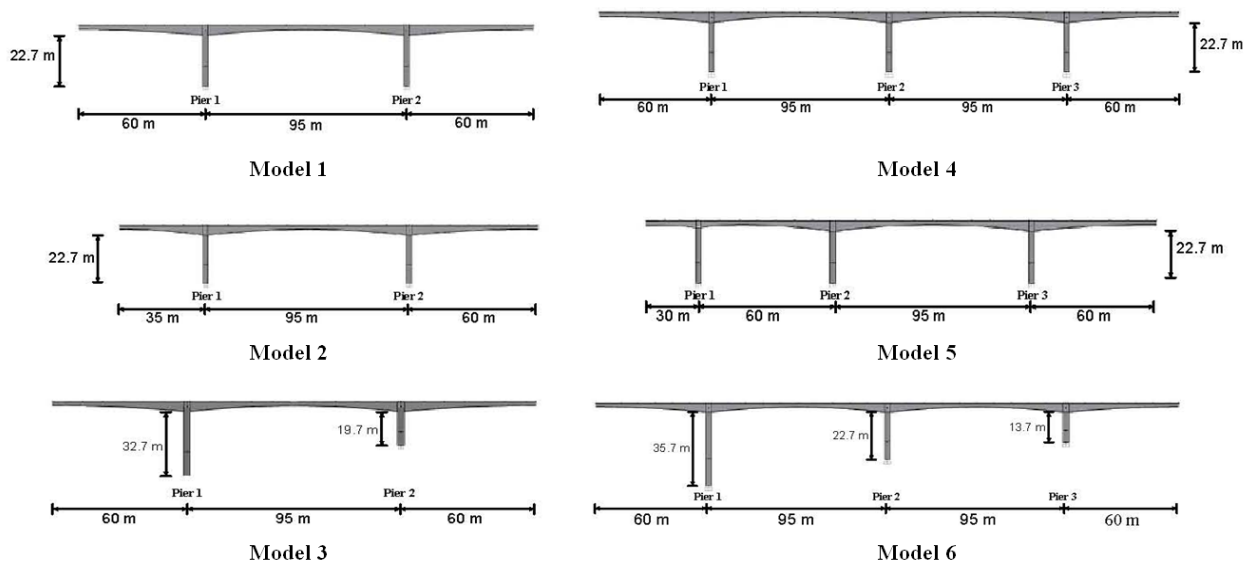


Figure 2.2. Three and four spans generated bridge models

Table 2.1. Relative stiffness of piers in different models with their dynamic specification in each direction

Models no.	Longitudinal Direction			Transverse Direction			First Longitudinal Mode		First Transverse Mode	
	Pier No. 1	Pier No. 2	Pier No. 3	Pier No. 1	Pier No. 2	Pier No. 3	Period (Sec)	MPR*	Period (Sec)	MPR*
1	1.00	----	1.00	1.00	----	1.00	1.129	0.99	1.692	0.88
2	1.00	----	1.01	1.00	----	1.01	1.080	0.99	1.591	0.89
3	1.00	----	5.33	1.00	----	4.22	1.115	0.99	1.688	0.86
4	1.00	1.00	1.00	1.02	1.00	1.02	1.308	0.99	1.886	0.87
5	1.00	2.48	2.49	1.00	4.38	4.42	1.186	0.99	1.752	0.88
6	1.00	4.65	22.19	1.00	3.79	14.17	1.265	0.97	1.902	0.81

*MPR : Mass Participation Ratio

3. MODELING OF THE BRIDGES

In order to investigate nonlinear behavior of described highway bridges, their three dimensional models have been built up in OpenSees. The deck has been modeled with elastic elements due to post tensioning force. In order to simulate pier's nonlinear behavior, concentrated plastic hinge with fiber

section was used at both ends of the piers (see Fig. 3.1). Plastic hinge length has been calculated by SDC 2006 for rectangular sections. In all elastic elements, modulus (E) and shear modulus (G) was considered according to SDC 2006 recommendation. Also bridge mass was assigned through lumped masses as it is shown in Fig. 3.1.

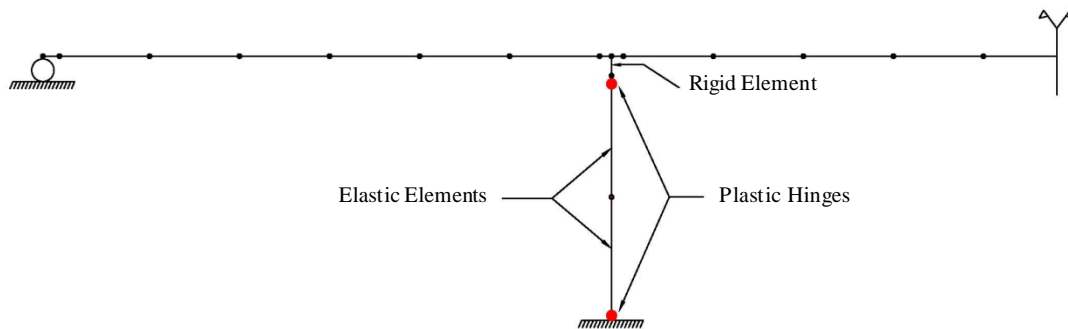


Figure 3.1. Finite element models of deck and piers

In pier section, confined and unconfined concrete behaviors have been assigned based on Mander et al. (1988) model (see Fig. 3.2). It is noteworthy that the compression strength of concrete in the piers is 30 MPa. Also steel specifications of “A706/A706M (Grade 60/Grade 400)” according to SDC 2006 were used for reinforcement. In order to consider limit state in material behavior, the generated stress-strain response has been limited. The concrete fibers strain limit state in core and cover have been considered 0.013 and 0.006, respectively. Moreover, the strain limit state of about 2% in compression and 6% in tension has been considered for rebar material.

Viscous Rayleigh damping of 2% and P-Delta effect was included in nonlinear analysis of bridge. However soil and structure interaction at foundation level of models was neglected in agreement to SDC 2006 recommendations of ordinary bridges, interaction between deck and abutment was modeled as it shown in Fig. 3.3. In this figure, abutment contains a rigid element which is supported with three springs in each direction at its both ends. “HyperbolicGapMaterial” was used for elastic-perfectly-plastic (EPP) backbone curve of longitudinal response which is reported by SDC 2006 (Wilson and Elgamal (2006)).

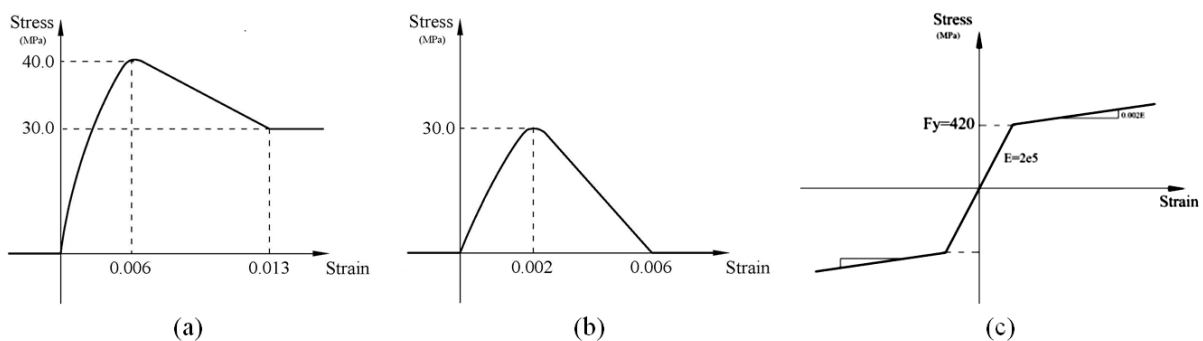


Figure 3.2. Nonlinear behavior curve of (a) confined concrete, (b) un-confined concrete (Mander et al. 1988), and (c) steel behavior of rebar

At the presented model, the effect of backfill and wing wall on transverse direction is also considered. In order to simulate these effects, transverse spring's specifications are defined in proportion to longitudinal response. Also For vertical direction, elastic no tension spring (ENT) is assigned at each end of the rigid link based on bearing pads stiffness (Aviram et al. (2008)).

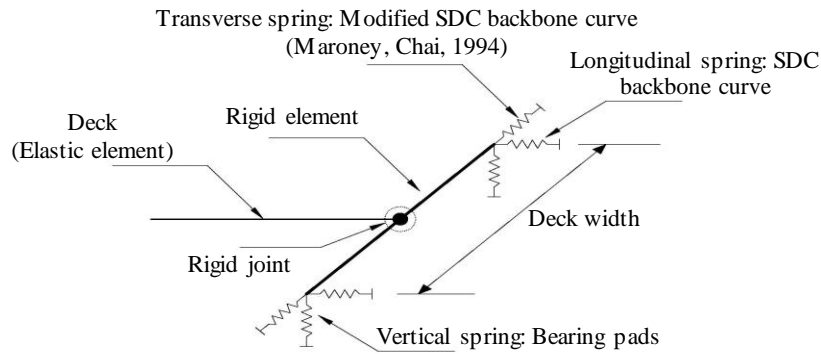


Figure 3.3. Components of “simplified” mechanism for abutment modeling

4. INPUT GROUND MOTIONS

Table 3.1 provides input ground motions in this study which have selected from PEER1 NGA database and recorded on soil type II site. Since forward directivity pulse can be observed only in fault normal direction, the near fault components in each station have been rotated to fault normal and parallel orientation. The near fault records have been adopted with wide range of pulse periods to cover first mode vibration period of six different bridges.

To have engineering judgment regarding to seismic performance of high way bridge, input accelrograms in far fault set should be scaled to actual seismic ground motion in DBE level. The acceleration components should be scaled in such a manner that square root of the sum of the squares (SRSS) from each pairs of the accelrograms with damping ratio 5 percent and a vibration period in the range from 0.2T and 1.5T seconds not fall below 1.3 times the site specific design spectrum. But for near fault earthquakes this procedure couldn't be applied, because in this way the near fault pulses would be attenuated unrealistically. Following, in this study the method which is proposed with ASCE7-2010 was used for scaling. According to this provision, at sites within 3 miles (5 km) of the active fault that controls the hazard, each pair of components shall be rotated to the fault-normal and fault-parallel directions of the causative fault and shall be scaled so that the average of the fault-normal components is not less than the MCE response spectrum for the period range from 0.2T to 1.5T. In this way the average of scale factors in two record sets of far fault and near fault earthquakes would be closer especially for ordinary structures with natural period around 1.00 second. Additionally to have realistic comparison between two types of ground motions and their effect on seismic behavior of bridges, far fault records are also normalized to MCE level. In both scaling procedure the 5% damping acceleration spectrum of the soil type II in DBE and MCE levels was chosen based on Iranian earthquake code 2800.

Fig. 4.1 (left) shows the averages of SRSS near fault and far fault spectrum before scaling with standard spectrums. It can be inferred that, in period range of structures which is about 1.0-2.0 sec, there is significant difference between near fault and far faults graphs. Fig. 4.1 (right) shows the SRSS averages of near fault and far faults spectrums after scaling for case study (model No.1). The figure shows that their difference stayed almost in the same value after scaling both types of ground motions in the period range of this model. From the figure, the average acceleration spectrum of far fault set which is scaled to MCE level has higher amplitude than others, however near fault spectrum approaches to MCE level of far fault spectrum in the long period region. This could be explained by the role of near fault ground motion records especially in long period systems. Scale factors of ground motions in different levels in case study model (model No. 1) have been shown in Table 3.1. The average of scale factors for far fault earthquake scaled into DBE and MCE levels are 3.08, 4.62 and

¹ Pacific Earthquake Engineering Research Center

for near fault earthquakes is 2.41. Comparing the values shows that, scale factors for all near fault records are less than far fault ground motions in MCE level.

Table 3.1. Far fault and near fault sets of ground motions

Record No.	Name / Station	Year	M	PGA	PGV	Pulse Period (Sec.)	Distance to Source (km)	Scale Factor	
				g	cm/s			DBE	MCE
Far fault ground motions									
1	Hector Mine / Hector	1999	7.1	0.34	42	----	----	3.433	5.153
2	Kobe, Japan / Nishi - Akashi	1995	6.9	0.51	37	----	----	3.252	4.881
3	Chi-Chi, Taiwan / CHY028	1999	7.6	0.79	72	----	----	1.676	2.516
4	Manjil, Iran / Abhar	1990	7.4	0.51	54	----	----	2.491	3.738
5	Chi-Chi, Taiwan / TCU045	1999	7.6	0.51	39	----	----	3.017	4.528
6	Friuli, Italy / Tolmezzo	1976	6.5	0.35	31	----	----	4.520	6.784
7	Chi-Chi, Taiwan / TCU095	1999	7.6	0.53	56	----	----	2.122	3.185
8	Northridge/Castaic - Old Ridge Route	1994	6.69	0.49	47	----	----	2.245	3.369
9	Northridge / Beverly Hills - Mulhol	1994	6.69	0.51	33	----	----	3.335	5.006
10	Victoria, Mexico / Cerro Prieto	1980	6.33	0.57	27	----	----	4.669	7.009
Near fault ground motions									
1	Coalinga-05 / Oil City	1983	5.8	0.87	41	0.7	4.1	----	4.163
2	Morgan Hill / Coyote Lake Dam	1984	6.2	0.81	62	1	0.53	----	2.753
3	Chi-Chi- Taiwan-03 / CHY080	1999	6.2	0.47	70	1.4	22.37	----	2.439
4	Northridge-01 / LA Dam	1994	6.7	0.58	77	1.7	5.92	----	2.217
5	Chi-Chi- Taiwan / CHY006	1999	7.6	0.31	65	2.6	9.77	----	2.626
6	Cape Mendocino / Petrolia	1992	7	0.61	82	3	8.18	----	2.082
7	Northridge-01 / Jensen Filter Plant	1994	6.7	0.52	67	3.5	5.43	----	2.548
8	Chi-Chi- Taiwan / TCU076	1999	7.6	0.30	64	4	2.76	----	2.667
9	Bam / Bam	2003	6.5	0.80	121	4.3	1.0	----	1.411
10	Landers / Lucerne	1992	7.3	0.72	140	5.1	2.19	----	1.219

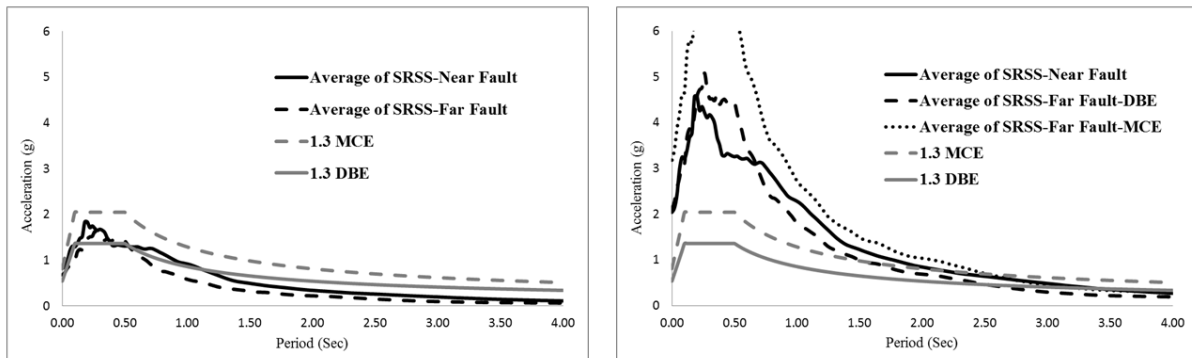


Figure 4.1. Average of SRSS spectrum of near fault earthquakes before scaling (Left) and after that (Right)

5. DESCRIPTION OF DIFFERENT SCENARIOS FOR INPUT MOTIONS

It is known that the observation of forward directivity effects depends on source-to-site geometry. Several source-to-site geometry parameters have been used in past to predict directivity effects at a site. The parameters like; distance from the fault, amount of rupture between the fault and the site and the angle between the strike of the fault and line joining epicenter and the site. However seismic performance of structures under pulse like ground motions can be investigated only in extreme

scenario which is fault normal component, fault normal component can be parallel to transverse or longitudinal direction of highway bridges (See Fig. 5.1). Herein, these two extreme scenarios have been described by FN in T and FN in L. Also far fault ground motions scenarios in two levels of DBE and MCE have been named as FF DBE and FF MCE, respectively.

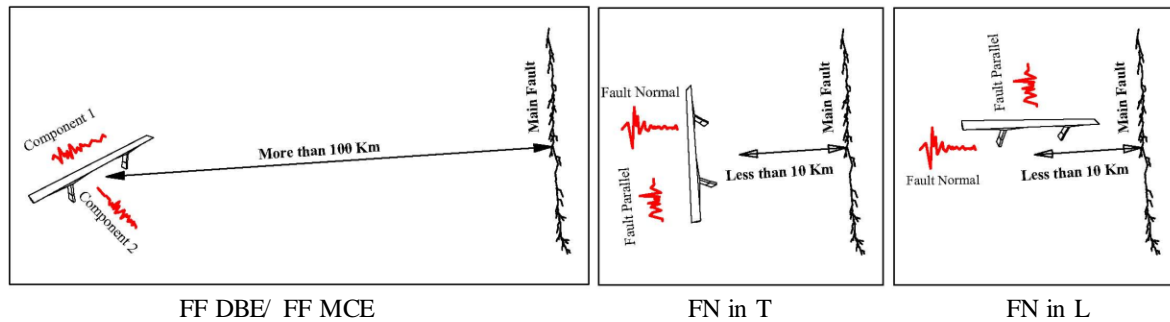


Figure 5.1. Schematic presentations for different scenarios

6. RESULT OF ANALYSIS

6.1. Drift Ratio In Piers

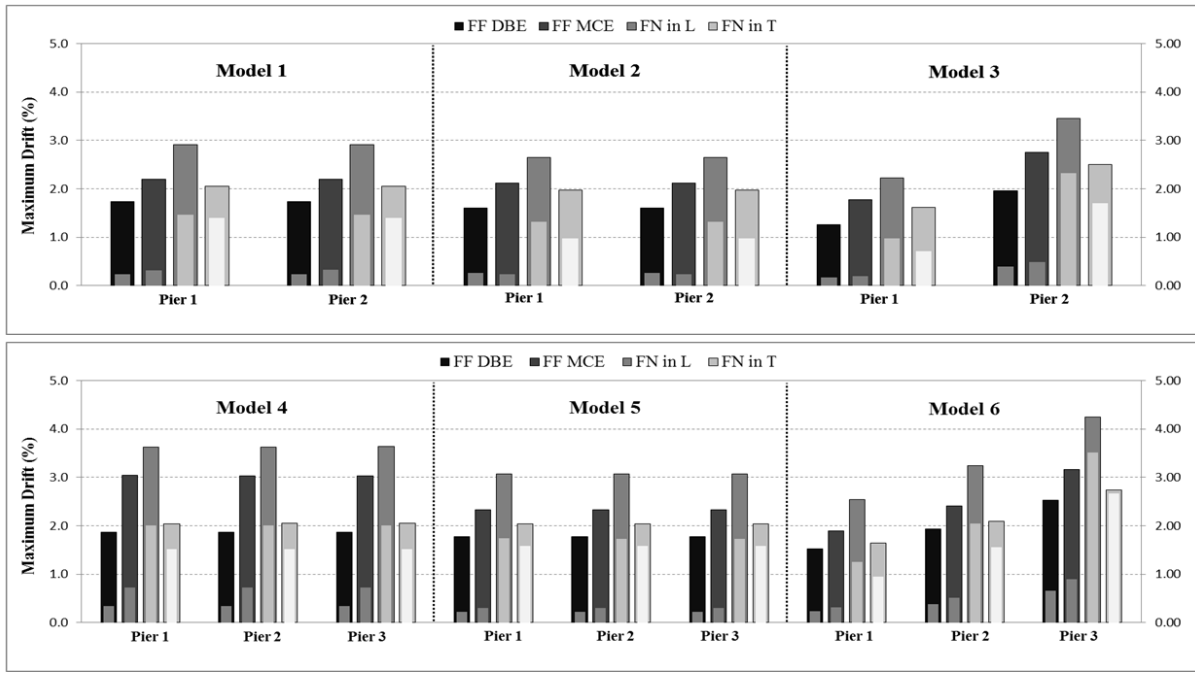
The obtained results from 240 nonlinear dynamic time history analyses on three dimensional models of six different high way bridges are shown in Fig. 6.1. This figure shows the average values of maximum drift ratios in longitudinal and transverse directions of piers with their variances which are shown by central pale color strip. It can be observed that under near fault parallel components, maximum drift ratio of bridges are between FF DBE and FF MCE scenarios. However the scaling factors in far fault records (FF DBE and MCE) are higher than near fault ones, the maximum drift ratios of fault normal components are higher than far fault scenarios. The average of maximum drift ratios under near fault ground motions is about 1.5 to 2.2 times of same parameter under DBE level of far fault earthquakes. Moreover, even under far fault earthquakes which are scaled to MCE level (FF MCE), the ratio is about 1.0 to 1.3. In irregular bridges particularly those with irregularity in height of piers, the ratio increases into the highest value. Also Fig. 6.1 indicates that transverse direction of bridges under near fault ground motions is more susceptible to suffer damage than longitudinal direction.

The different effect of near fault ground motions on the bridges can be also recognized from dispersion of maximum drifts in the piers. From Fig. 6.1, the dispersions of the responses under both near fault earthquake components (fault normal and fault parallel) are so much higher than far fault ones in both DBE and MCE levels. The variance of maximum drift under near fault ground motion is about 5.0 to 9.0 times of DBE and is about 1.5 to 5.5 times of MCE scenarios.

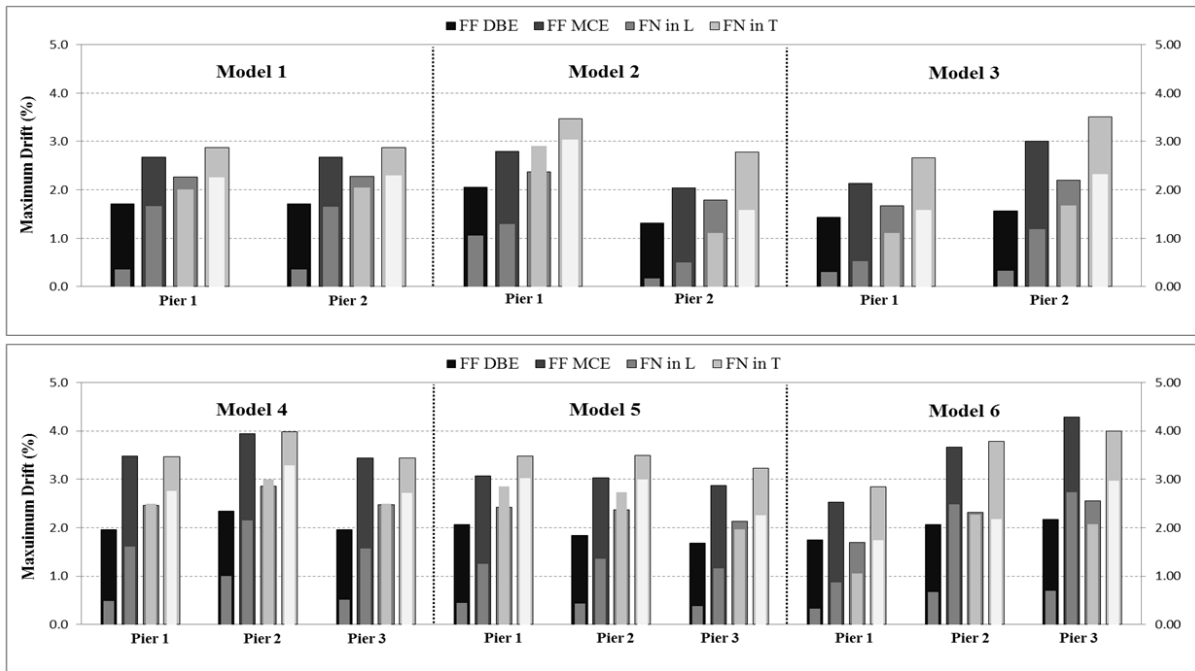
Details of analysis and the collapse criteria of piers reveal that although design procedure of AASHTO provision can predict the demands of far fault earthquakes, it couldn't cover the seismic demands of near fault records properly. Consequently, most of the near fault earthquakes could be able to collapse the bridge structures, particularly the irregular ones in pier's height (Model 3 and 6).

6.2. Input And Hysteretic Energy Trade of

Fig. 6.2 shows different energy time history and hysteretic diagram of piers in case study bridge (model No. 1) under near fault and far fault ground motions in longitudinal direction. In energy time history graphs, total input energy (E_i), hysteretic energy of Piers (W_{H-Pier}), hysteretic energy of abutments (W_{H-Abut}) and kinematic energy (W_K) are shown under record No.6 (FN) and record No.10 (FF) in two level DBE and MCE. In addition, plastic hinge hysteresis diagrams under different scenarios are shown in this figure.



(a)



(b)

Figure 6.1. Pier drifts of bridges under different scenarios; (a) longitudinal direction, (b) Transverse direction

The presented results show that the maximums of drift and velocity time histories of fault normal component have been peaked at the same. The peak value of velocity time history in this component is about 1.16 and 0.77 times of far fault ground motion in DBE and MCE levels, respectively. Furthermore, energy time history of pulse like ground motion, input energy and consequently hysteretic energy reach to maximum values in a very short time (in this case it is about $\frac{1}{4}$ times of far fault one) and it causes piers to dissipate large amount of energy in short time. Consequently, this phenomenon results in larger deformation demand in piers, which is shown in hysteretic diagram.

The hysteretic response of a sample plastic hinge under pulse-like ground motion shows fewer numbers of recurring loops with extreme value of rotation comparing with the far fault results. This

configuration results dissipated energy reaches to 32% of total input energy in this direction, whereas the values of far fault record in both levels are about 45%. Consequently, larger quota of input energy will absorb through the abutment. In this way, hysteretic behavior of abutments shows significantly higher value of ductility demand under near fault motions comparing with the far fault outcomes. The ratio of abutment energies to total input energy in longitudinal is about 0.46, however the ratios for far fault ones are about 0.30 in both levels of motions. The values obviously show the participation of abutments in structural response under near fault ground motions due to large deformation. Also, hysteretic diagram shows near fault pulses increase the demand of ductility, therefore the high way bridges require further ductile capacity. These characteristics of near fault pulses and their effects have not been considered in modern design procedure.

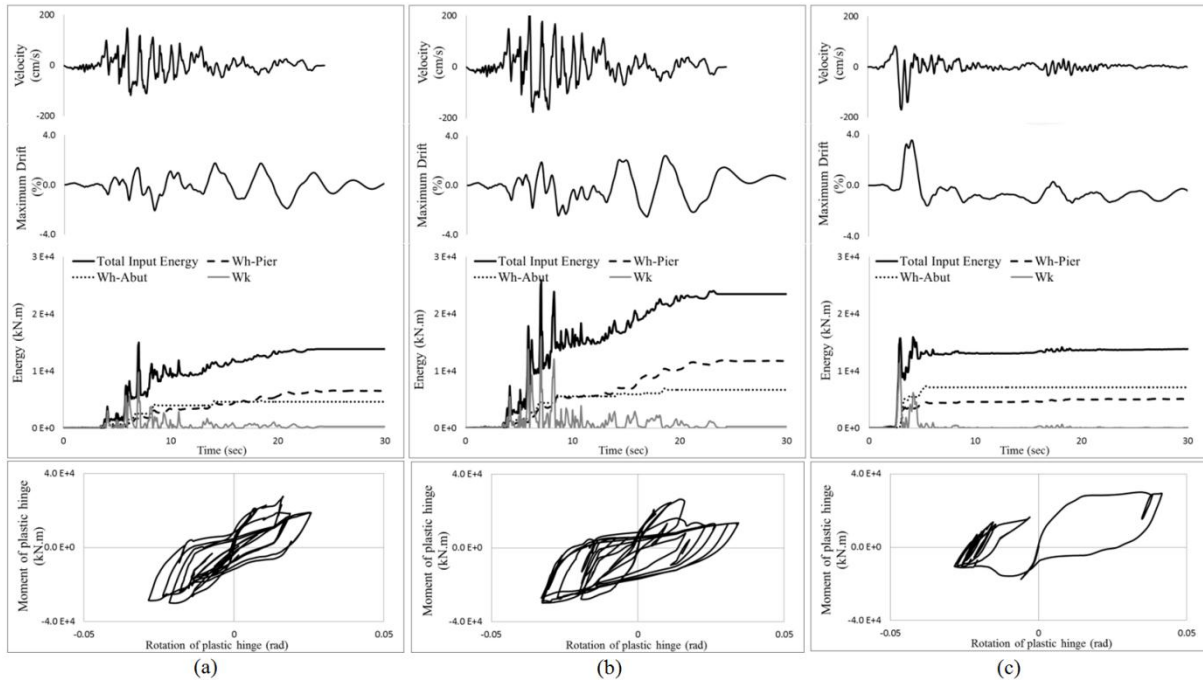


Figure 6.2. Velocity record No 6. ((a) FF DBE, (b) FF MCE) and No.10 ((c) FN in T) and their corresponding energy time history and hysteretic diagram of pier in model No. 1 in longitudinal direction

7. CONCLUSION

In this study seismic performance of a case study framed box girder Highway Bridge has been investigated by using a three dimensional precise model. A basic bridge and 5 other generated bridges have been designed and 240 nonlinear time history analyses carried out. The sample bridges have been designed in such way that a wide range of irregularity has been covered in agreement with AASHTO 2007 provision. Also, four different scenarios of near fault ground motions have been compared with the far fault ones in DBE and MCE levels. The scenarios have been chosen based on fault rupture direction regarding to bridge position in order to study forward directivity pulses in each direction of piers. Seismic demand parameters like drift ratio, hysteretic energy and input energy have been computed in longitudinal and transverse directions of regular and irregular models. The obtained results are summarized as follow:

1. The results show under near fault pulses, seismic drift of piers is about 2.0 times of far fault records in DBE level and 1.3 times of same records in MCE level, These results have been derived when the average of scale factor for near fault records are about 0.8 and 0.5 times of DBE and MCE levels, respectively.
2. Larger amount of dispersion is observed in seismic response of bridges under scaled near fault records.

3. The hysteretic energies under near fault earthquakes are lower than far fault ground motions. The reason is in hysteretic loops configurations which contain fewer numbers of recurring loops and having loops with extreme value of rotation under near fault ground motion.
4. The results indicate the characteristics of near fault pulses and their effect have not been considered in modern design provisions for bridges.

REFERENCES

- Alavi, B., and Krawinkler, H. (2001). Effects of near-fault ground motions on frame structures. Earthquake Engineering Center, Report No, 138, Department of Civil Engineering, Stanford University.
- American Association of State Highway and Transportation Officials (2007). AASHTO Standard Specifications for Highway Bridges, AASHTO, Washington, D.C.
- American Society of Civil Engineers (ASCE). (2005). Minimum Design Loads for Buildings and Other Structures, ASCE/SEI 7, USA.
- American Society of Civil Engineers (ASCE). (2010). Minimum Design Loads for Buildings and Other Structures, ASCE/SEI 7, USA.
- Aviram, A., Mackie, K.R., and Stojadinović, B., (2008). Guidelines for Nonlinear Analysis of Bridge Structures in California. Pacific Earthquake Engineering Center (PEER), Report No. 2008/03, August.
- Bertero, V.V., Mahin, S.A., and Herrera, R.A., (1978). A Seismic Design Implication of Near-fault San Fernando Earthquake Records. *Earthquake Engineering and Structural Dynamics* **6**, 31-34.
- Caltrans (2006). Caltrans Seismic Design Criteria version 1.4. California Department of Transportation, Sacramento, California.
- Iervolino, I., Cornell, C. A., (2008). Probability of Occurrence of Velocity Pulses in Near-Source Ground Motions. *Bulletin of the Seismological Society of America*. **98:5**, 2262–2277.
- Iranian Code of Practice for Seismic Resistant Design of Buildings -Standard (2005). No.2800-05 (3rd Edition).
- Kalkan, E., and Kunnath, S. K., (2006). Effects of Fling Step and Forward Directivity on Seismic Response of Buildings. *Earthquake Spectra*. **22: 2**, 367–390.
- Liao W.I., Loh, C.H., Wan, S., Jean, W.Y., Chai, J.F., (2000). Dynamic responses of bridges subjected to near-fault ground motions. *Journal of the Chinese Institute of Engineers*. **23:4**, 455–64.
- Mander J. B., Priestley, M. J. N., and Park, R., (1988). Theoretical Stress-Strain Model for Confined Concrete. *Journal of Structural Engineering*, ASCE. **114:8**, 1804-1849 .
- PEER Strong Motion Catalog. <http://peer.berkeley.edu/smcat>. Web page-2012-March.
- Phan, V., Saiidi, S., Anderson, J., and Ghasemi, H., (2007). Near Fault Ground Motion Effect on Reinforced Concrete Bridge Columns. *Journal of Structural Engineering*, ASCE. **133:7**, 982-989, July.
- Sadrossadat Zadeh, and Saiidi S., (2007). Pre-test Analytical Studies of NEESR-SG 4-Span Bridge Model Using OpenSees. Center of Civil Engineering Earthquake Research. University of Nevada, Reno, USA, Report No. CCEER-07-3, February.
- Somerville, P. G. (2003). Characterizing Near-Fault ground motions for the design and evaluation of bridges. *Pacific Earthquake Engineering Research Center (PEER)*.
- Wilson, P. and Elgamal, A. (2006). Large scale measurement of lateral earth pressure on bridge abutment back-wall subjected to static and dynamic loading. *Proceedings of the New Zealand Workshop on Geotechnical Earthquake Engineering*. University of Canterbury, Christchurch. New Zealand: 307-315.